# Anodic Fragmentation of Catharanthine and Coupling with Vindoline. Formation of Anhydrovinblastine

Ibro Tabakovic* and Esmir Gunic

*Department of Chemistry, University of Minnesota, Minneapolis, Minnesota 55455*

Ivan Juranic

*Faculty of Chemistry, University of Belgrade, 11000 Belgrade, Yugoslavia*

*Received November 12, 1996*[⊗]

The anodic oxidation of catharanthine (Cath) in the presence of vindoline (Vind) performed in $MeCN-Et_4NClO_4$ at a controlled potential yields (16′*S*)- and (16′*R*)-anhydrovinblastine (AVBL) in s 4.3:1 ratio. The favorable stereoselectivity found at room temperature is rationalized by proposing the coupling of generated dication **1a**$^{++}$ and Vind at the electrode surface. The mechanism of the overall fragmentation/coupling reaction was studied using electrochemical techniques and the technique of homogeneous redox catalysis. It was concluded that the rate-determining step in the overall reaction is the first electron transfer leading to Cath$^{\bullet+}$. MO calculations support the proposed mechanism and provide the evidence that C16−C21 bond fragmentation is a homolytic process.

## Introduction

The dimeric Catharanthus alkaloids vinblastine and vincristine isolated from the leaves of the Madagascan periwinkle *Catharanthus roseus*[1] present themselves as challenging targets to the synthetic chemist. These two alkaloids are efficacious, clinically useful anticancer reagents which are used routinely for the treatment of a number of human cancers.[2] Since these natural products are present in the plant material in very low concentrations, numerous research groups have been actively engaged in developing methods for their synthesis[3] by coupling the alkaloids catharanthine (Cath) and vindoline (Vind) which are synthetically available.[4] This basic idea relies on the biogenetic consideration that binary indole-indoline alkaloids are formed in plants by coupling of Cath and Vind[5] leading to the key intermediate anhydrovinblastine (AVBL) which can be transformed to vinblastine and vincristine (Scheme 1).

This process was efficiently carried out by the Polanovski reaction through coupling of trifluoroacetylated catharanthine *N*-oxide with vindoline.[6]

These studies had considered this reaction as a chemical "mimic" for the peroxidase enzyme involved in the enzyme-catalyzed coupling of Cath and Vind.[6] However, it was concluded that catharanthine *N*-oxide is not accepted as a precursor in the enzymatic process to AVBL, so a different "activation" of Cath by the enzyme is involved.[7] The mechanism of the catharanthine *N*-oxide and vindoline fragmentation/coupling process by trifluoroacetic anhydride was studied by low temperature NMR.[8] The coupling of catharanthine and vindoline was carried out under $Fe^{3+}$ oxidative conditions[9] followed by reduction with sodium borohydride. While there have been significant advances following other approaches,[10] the oxidative fragmentation/coupling route to anhydrovinblastine remains a topic of interest. A new way of effecting fragmentation of Cath at C16−C21 based on the electron transfer reactions was discovered.[11] We have reported that an anodic oxidation can be used to synthesize anhydrovinblastine in good yield and stereoselectivity by coupling of catharanthine and vindoline, even at room temperature.[12]

The oxidative fragmentation of Cath at the C16−C21 bond is an important process in both the chemical synthesis and biosynthesis of AVBL.[1,3] We have shown recently that the anodic oxidation of Cath in methanol to Cath$^{\bullet+}$ and fragmentation of C16−C21 bond is occurring through a concerted mechanism.[13]

In the present paper the oxidative fragmentation of Cath leading to pivotal intermediate **1a**$^{++}$ and coupling with Vind has been investigated by voltammetric techniques. It was found that the rate-determining step in the overall fragmentation/coupling reaction is the first electron transfer. MO calculations support the homolytic mode of fragmentation. The steroselectivity and mech-

[⊗] Abstract published in *Advance ACS Abstracts,* February 1, 1997.

(1) Blasko, G.; Cordell, G. A. Isolation, Structure Elucidation and Biosynthesis of the Bisindole of Catharanthus. In *The Alkaloids*; Brossi, A., Suffness, M., Eds.; Academic Press, New York: 1990; Vol. 37, p 12.

(2) Neus, N.; Neus, M. N. The Therapeutic Use of Bisindole Alkaloids from Catharanthus. In *The Alkaloids*; Brossi, A., Suffness, M., Eds.; Academic Press: New York, 1990; Vol. 37, p 232.

(3) Kuehne, M. E.; Marko, I. Synthesis of Vinblastine Type Alkaloids. In *The Alkaloids*; Brossi, A., Suffness, M., Eds.; Academic Press: New York, 1990; Vol. 37, p 77.

(4) (a) Raucher, S.; Bray, B. L. *J. Org. Chem.*, **1985**, *50*, 3236. (b) Szantay, C.; Bolcski, H.; Gasz-Baitz, E. *Tetrahedron* **1990**, *46*, 1711. (c) Andriamialisoa, R. Z.; Langlois, N.; Langlois, Y. *J. Org. Chem.* **1985**, *50*, 961.

(5) Scott, A. I.; Gueritte, F.; Lee, S. L. *J. Am. Chem. Soc.* **1978**, *100*, 6253.

(6) (a) Langlois, N.; Gueritte, F.; langlois, Y.; Potier, P. *J. Am. Chem. Soc.*, **1976**, *98*, 7017. (b) Kutney, J. P.; Hibino, T.; Jahngen, E.; Okutani, T.; Ratcliffe, A. H.; Treasurywaka, A. M.; Wunderly, S. *Helv. Chim. Acta* **1976**, *59*, 2858.

(7) Kutney, J. P. *Acc. Chem. Res.* **1993**, *26*, 559 and the references therein.

(8) Sundberg, R. J.; Gadamesetti, K. G.; Hunt, P. J. *Tetrahedron* **1992**, *48*, 277.

(9) (a) Vukovic, J.; Goodbody, A. E.; Kutney, J. P.; Misawa, M. *Tetrahedron* **1988**, *44*, 325. (b) Balazs, N.; Szantay, C., Jr.; Boleski, H.; Szantay, C. *Tetrahedron Lett.* **1993**, *34*, 4397.

(10) (a) Kutney, J. P. *Nat. Prod. Rep.* **1990**, *7*, 87. (b) Kuehne, M. E.; Matson, P. A.; Bornmann, W. G. *J. Org. Chem.* **1991**, *56*, 513. (c) Magnus, P.; Stamford, A.; Ladlow, M. *J. Am. Chem. Soc.* **1990**, *112*, 8210.

(11) (a) Sundberg, R. J.; Desos, P.; Gadamesatti, K. G.; Sabat, M. *Tetrahedron Lett.* **1991**, *32*, 3035. (b) Sundberg, R. J.; Hunt, P. J.; Gadamesatti, K. G. *J. Org. Chem.*, **1991**, *56*, 8210.

(12) Gunic, E.; Tabakovic, I.; Gasic, M. J. *J. Chem. Soc., Chem. Commun.* **1993**, 1496.

(13) Tabakovic, I.; Gunic, E.; Gasic, M. J. *J. Chem. Soc., Perkin Trans. 2* **1996**, 2741.

S0022-3263(96)02112-3 CCC: $14.00 

**Scheme 1**

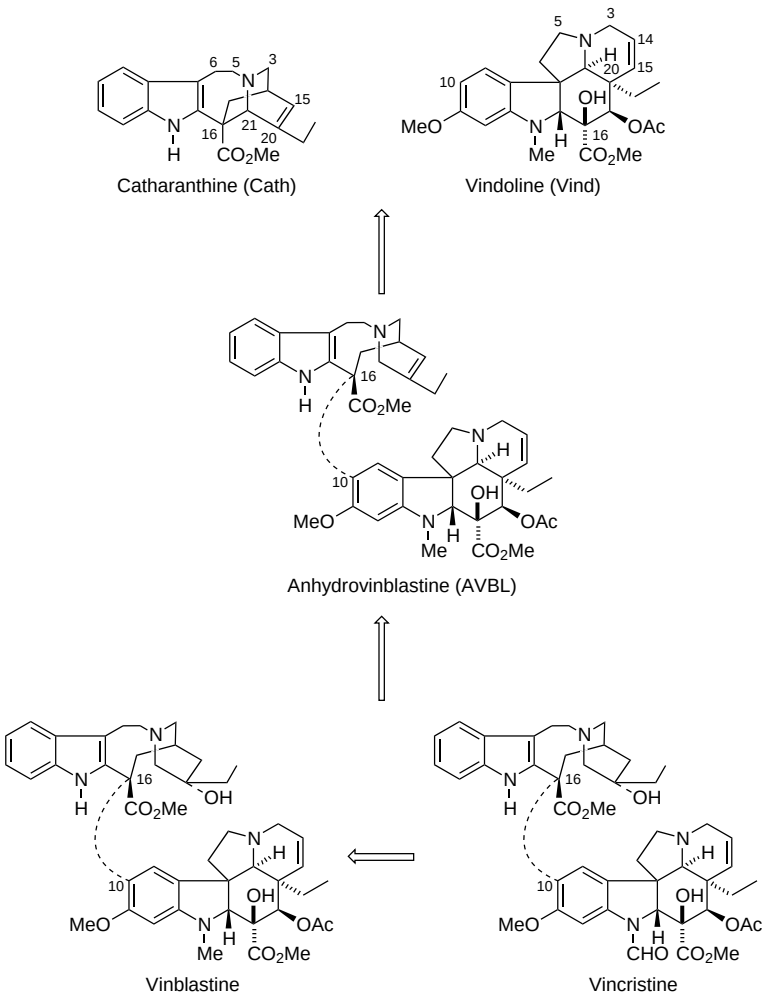


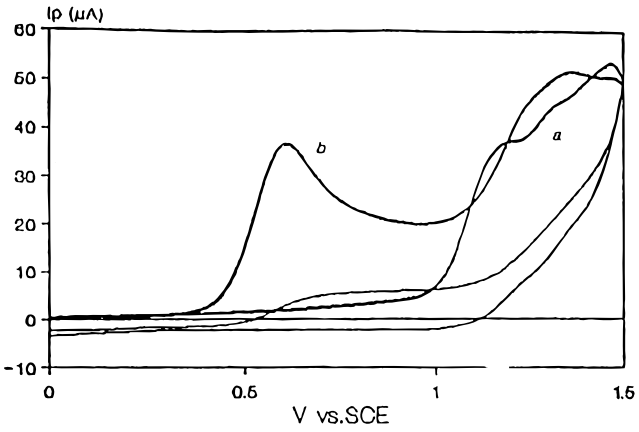


**Figure 1.** Top: (a) Cyclic voltammogram of $CathH^+$ (1 mM) in MeCN−0.1 M $Et_4NClO_4$ at GCE; $v$ = 100 mV/s; (b) plus 2,6-lutidine (4 mM).

anism of the coupling between catharanthine and vindoline leading to anhydrovinblastine was discussed.

## Results and Discussion

**Direct Oxidation of Catharanthine.** The cyclic voltammogram of the catharanthine hydrochloride salt ($CathH^+$) presented in Figure 1 shows two anodic peaks at 1.20 and 1.30 V vs SCE, respectively. When the cyclic voltammogram was run in the presence of 2,6-lutidine the new peak at 0.60 V vs SCE appeared due to the oxidation of Cath as a free base. The height of the peak current ($i_p$ = 36.1 $\mu$A) corresponds to the two electron oxidation (see text) in $Et_4NClO_4$−MeCN solution.

The cyclic voltammograms run at sweep rates from 0.02 to 40 V/s are all characterized by an anodic wave showing a well-defined current maximum but no cathodic wave on the reverse scan even at high sweep rates. Under the experimental conditions this wave is irreversible and broad. The peak width ($E_p - E_p/2$) varies from 90 mV at 20 mV/s to 100 mV at 200 mV/s, showing[14] that the reaction is under the rate control of the first electron transfer. The average value of the transfer coefficient obtained from the peaks widths[15] of the voltammograms at seven sweep rates ($\alpha$ = 0.49) is in fairly good agreement with the transfer coefficient obtained from the Eplog $v$ slope[14,15] ($\alpha$ = 0.53). The peak currents have a linear dependence on the square root of the sweep rates, indicating that the overall process is diffusion controlled.

The diffusion coefficient for Cath ($D = 1.4 \times 10^{-5}$ cm$^2$/s) was obtained from analysis of the chronoamperometric $i-t$ transient according to the following equation[16]

$$it^{1/2} = n\mathrm{FAC}(D/\pi)^{1/2}$$

At the applied potential (0.8 V vs SCE) the product of the current and the square root of the time was observed

(14) Nadjo, L.; Saveant, J.-M. *J. Electroanal. Chem.* **1973**, *48*, 113.
(15) Nicholson, R. S.; Shain, I. *Anal. Chem.* **1964**, *36*, 706.
(16) Adams, R. N. Electrochemistry at Solid Electrodes; Marcel Dekker: New York, 1969.

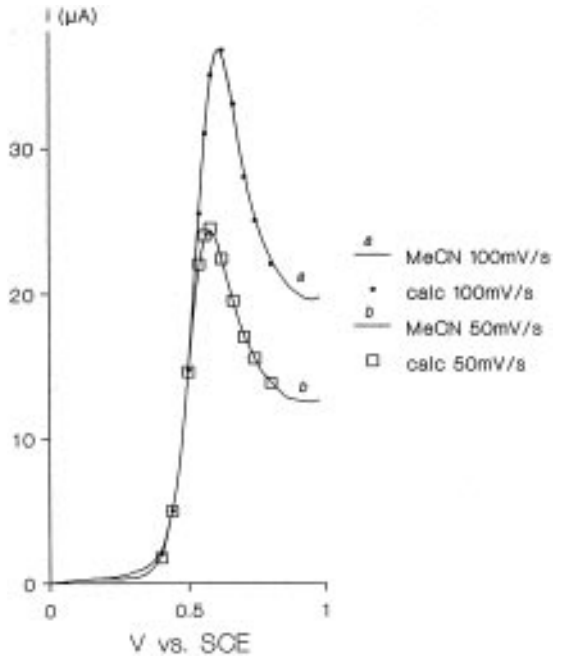


**Figure 2.** Calculated and experimental voltammograms of CathH$^+$ (1 mM) in MeCN−0.1 M $Et_4NClO_4$ plus 2,6-lutidine (4 mM) at GCE. The calculated points are obtained using $\alpha = 0.51$, $D = 1.4 \times 10^{-5}$ cm$^2$/s, $n = 2$, $A = 0.071$ cm$^2$.

to be constant from 2 to 6 s. The area of the electrode ($A = 0.071$ cm$^2$ ) was calibrated with ferrocene for which the diffusion coefficient is $D = 2.4 \times 10{-}5$ cm$^2$/s.[17]

The shape of the wave was analyzed by using the method of Nicholson and Shain[15] for irreversible electron transfer according to the following equation

$$i(t) = n\mathrm{FAC}\,(\pi Db)^{1/2}\,\chi\,(bt)$$

where $b = \alpha Fv/RT$ is the normalized sweep rate expressed in units of seconds$^{-1}$. The function $X$ ($bt$) contains all of the potential dependence, and it has been tabulated.[15] It follows that if the sweep rate $v$, the diffusion coefficient $D$, overall numbers of electrons $n$, and the transfer coefficient $\alpha$ are known, the shape of the entire wave can be completely defined. The calculated waves were shifted along the potential and current axes to match the values at the CV peaks, i.e. $t = t_o$ was defined to occur at $E_p = 0.6$ V vs SCE. A similar analysis of the shape of the CV for irreversible two-electron oxidation of alkyl metals was reported.[18] The results of these calculations indicated by the circles and squares in Figure 2 show very good agreement with the experimental cyclic voltammograms.

**Indirect Oxidation of Catharanthine.** We applied the redox catalysis method to study the fast ECE oxidation (Scheme 3, eqs 1−3) of Cath. The mediator used in the present study was ferrocene (Fc) with a standard potential ($E^o = 0.3$ V vs SCE) close enough to the oxidation potential of Cath for a measurable increase of the catalytic currents and also separated enough to avoid overlapping of the catalytic and direct oxidation wave of Cath. The successive steps involved in the redox catalytic process are represented in Scheme 2.

The catalytic effect is illustrated in Figure 3 where oxidized ferrocene, Fc$^+$, is generated reversibly at the

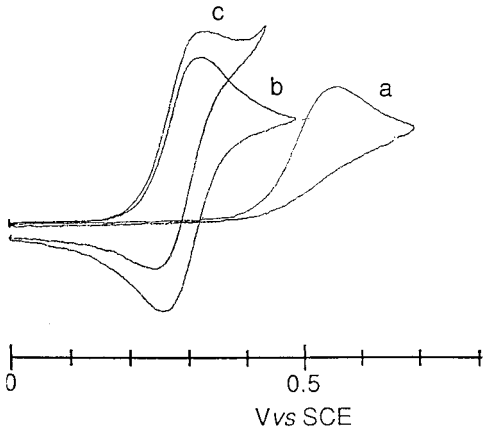


**Figure 3.** Homogeneous redox catalysis of Cath with Fc in MeCN−0.1 M $LiClO_4$ plus 2,6-lutidine (4 mM); $v = 100$ mV/s; Pt-anode (a) Cath (0.8 mM), (b) Fc (1.0 mM), (c) Fc (1 mM) plus Cath (4 mM).

**Scheme 2**

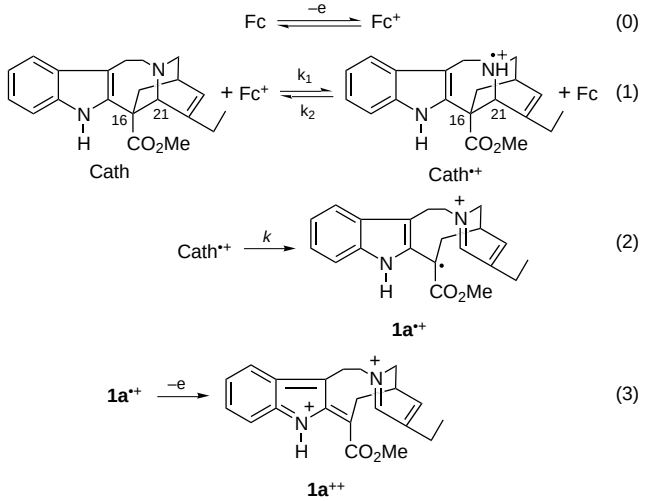


**Table 1. Homogeneous Redox Catalysis of the Oxidation of Catharanthine by Ferrocene**

| $C^*_{Fc}$ (mM) | $v$ (V/s) | $\gamma = 1.0$ $i_p/i_{pd}$ | $\gamma = 2.0$ $i_p/i_{pd}$ | $\gamma = 4.0$ $i_p/i_{pd}$ |
|---|---|---|---|---|
| 0.5 | 0.005 | 1.24 | 1.44 | 1.80 |
| | 0.010 | 1.16 | 1.23 | 1.48 |
| | 0.020 | 1.09 | 1.16 | 1.25 |
| | 0.050 | 1.05 | 1.05 | 1.09 |
| 1.0 | 0.005 | 1.43 | 1.68 | 2.04 |
| | 0.010 | 1.24 | 1.39 | 1.71 |
| | 0.020 | 1.16 | 1.25 | 1.42 |
| | 0.050 | 1.09 | 1.09 | 1.18 |
| 2.0 | 0.005 | 1.71 | 2.01 | |
| | 0.010 | 1.41 | 1.55 | |
| | 0.020 | 1.29 | 1.36 | |
| | 0.050 | 1.20 | 1.21 | |

electrode. The one electron reversible wave of Fc loses its reversibility upon addition of Cath to the solution. The excess current is due to the catalyzed oxidation of Cath by homogeneous redox catalysis through the Fc/Fc$^+$ couple, eq 0, followed by reactions 1−3. Radical cation **1a**$^{\bullet+}$ is formed close to the electrode surface, and since $k$ is large (vide infra) it will diffuse back and be oxidized at the electrode surface (reaction 3).

Table 1 summarizes the experiments carried out as a function of mediator concentration, $C^*_{Fc}$, the ratio of the bulk concentrations of Cath and Fc, $\gamma$, and the sweep rate $v$. The peak current ratio ($i_p/i_{pd}$, where $i_p$ and $i_{pd}$ are the

(17) Kuwana, T.; Bublitz, D. E.; Hoh, G. *J. Am. Chem. Soc.* **1960**, *82*, 5811.
(18) Klingler, R. J.; Kochi, J. K. *J. Am. Chem. Soc.* **1980**, *102*, 4790.

anodic peak currents for Fc with and without Cath, respectively) is useful for describing the quantitative features of the present homogeneous catalysis. The $i_p/i_{pd}$ value is largely dependent on the initial concentration of Fc and the excess factor $\gamma$. The overall homogenous catalytic oxidation of Cath can be controlled by reaction 1, reaction 2, or both reactions. When the overall reaction is controlled by C16−C21 fragmentation of $Cath^{\bullet+}$ (reaction 2) with reaction 1 as the preequilibrium state, the $i_p/i_{pd}$ value is independent of $C^*_{Fc}$ at constant $\gamma$.[19] The obvious dependence of the $i_p/i_{pd}$ value on the concentration of mediator at constant $\gamma$ in the present reaction rules out the possibility of this mechanism. When reaction 2 is fast compared to the reverse of reaction 1, the $i_p/i_{pd}$ value will increase with $C^*_{Fc}$ at constant $\gamma$,[19] and only then is it possible to obtain information about solution electron transfer. Therefore, the constant value of $k_1$ for a given $C^*_{Fc}$ range provides evidence that kinetic control is actually by forward reaction 1. A theoretical treatment of homogeneous redox catalysis as studied by cyclic voltammetry has been worked out for the ECE-type process.[19,20] Such a situation can be handled by calculating of $i_p/2\gamma i_{pd}$ (instead of $i_p/\gamma i_{pd}$) and using the working curves for $2\gamma$ (instead of $\gamma$). Data were obtained for four sweep rates (5, 10, 20, and 50 mV/s) at three concentrations of ferrocene (excess factor $\gamma$): 0.5 mM (1, 2 and 4), 1.0 mM (1, 2 and 4), and 2 mM (1 and 2).

To determine the rate constant for solution electron transfer (reaction 2) it is necessary to generate a working curve of $i_p/2\gamma i_{pd}$ vs log $\Lambda_1$. The quantity of $i_p/2\gamma i_{pd}$ is calculated, and $\Lambda_1 = k_1 C^*_{Fc}/(Fv/RT)$ is obtained by reference to theoretical working curves. Such working curves are available for the case of planar diffusion and the diffusion coefficients of all species being equal.[19] In the present case, the diffusion coefficient of the catalyst ferrocene is[17] $2.4 \times 10^{-5}$ cm$^2$/s while that of catharanthine is only $1.4 \times 10^{-5}$ cm$^2$/s as determined in this work. Thus it seemed prudent to prepare modified working curves (see Experimental Section) that included the effects of unequal diffusion coefficients.

The overall kinetics depend upon the forward reaction 1, as seen from the constancy of the $k_1$ values derived from the modified working curves. Thirty of the thirty-two conditions gave sufficient catalysis to determine $k_1$ reliably from the modified working curves resulting in a mean value of $k_1 = 38\ (\pm 10)\ M^{-1}\ s^{-1}$.

The 230 mV difference between the peak potentials of Fc and Cath suggests that $k_2$ is at the diffusion limit.

**Anodic Coupling of Catharanthine and Vindoline.** The cyclic voltammogram of Vind shows two anodic peaks at 0.77 and 0.95 V vs SCE, respectively (Figure 4). The first peak corresponds to the oxidation of tertiary amine moiety and the second peak to the indoline moiety. The protons liberated along the first wave attack other parent molecules and render them electroinactive, reducing the *n* value from 2 to 1. We have demonstrated that the oxidation of protonated vindoline at the potential of the second peak, followed by reduction at 0 V vs SCE, gave 10,10′-bis-vindoline in good yield.[21] By adding 2,6-lutidine the first wave increased and second wave disappeared. The cyclic voltammogram of the equimolar

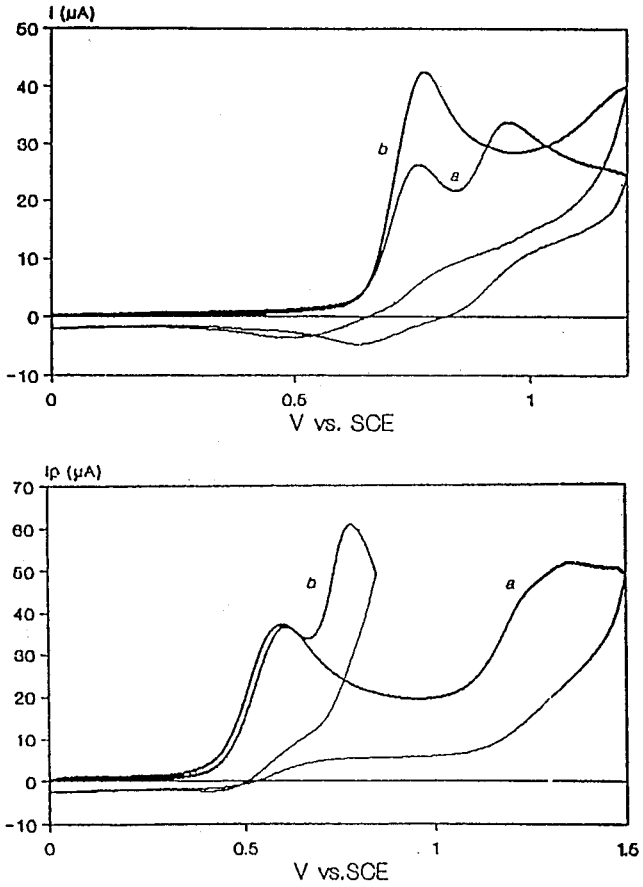


**Figure 4.** Top: (a) Cyclic voltammogram of Vind (1 mM) in MeCN−0.1 M $Et_4NClO_4$ at GCE; $v = 100$ mV/s, (b) plus 2,6-lutidine (4 mM) Bottom: (a) Cyclic voltammogram of $CathH^+$ (1 mM) in MeCN−0.1 M $Et_4NClO_4$ at GCE plus 2,6-lutidine (4 mM), (b) plus Vind (1 mM); $v = 100$ mV/s.

mixture of Cath and Vind (Figure 4) showed two anodic waves, one at 0.57 V vs SCE corresponding to the oxidation of Cath and the other at 0.78 V vs SCE due to the oxidation of Vind**.** The difference between the two potentials ($\Delta E_p = 210$ mV) enables the selective controlled potential oxidation of Cath in the presence of Vind. Importantly, the peak potential of Cath in the presence of Vind was shifted about 30 mV cathodically indicating the increase of the overall rate of the electrode reaction.

The electrochemical synthesis of anhydrovinblastine (AVBL) was performed by anodic oxidation of the equimolar mixture of Cath and Vind at a platinum gauze electrode (3 × 5 cm) in acetonitrile solution containing $Et_4NClO_4$ in a divided cell at controlled potential ($E =$ 0.6 V vs SCE). The electrolysis was monitored by HPLC and terminated after all starting material was consumed. The peaks in HPLC corresponding to Cath ($t_R = 5.13$ min) and Vind ($t_R = 4.38$ min) decreased during the electrolysis. A new peak at $t_R = 4.70$ min appeared corresponding to the $AVBL^+$ cation (Scheme 4) as the sole product by the end of the electrolysis. It has been demonstrated that $AVBL^+$ cation is sufficiently stable to be isolated and can be subjected to further chemical reactions.[22] Cyclic voltammograms under constant conditions were obtained as a function of charge passed. The results show that during controlled potential electrolysis, the oxidation wave decreases at a rate corresponding to the consump-

(19) Andrieux, C. P.; Blocman, C.; Dumas-Bouchiat, J. M.; M'Halla, F.; Saveant, J-M. *J. Electroanal. Chem.* **1980**, *113*, 19.
(20) Andrieux, C. P.; Blocman, C.; Dumas-Bouchiat, J. M.; M'Halla, F., Saveant, J.-M. *J Am. Chem. Soc.* **1980**, *102*, 3806.
(21) Tabakovic, I.; Tabakovic, K. *Tetrahedron Lett.* **1996**, *37*, 3659.
(22) Sundberg, R. J.; Bettiol, J. L.; Gadamesatti, K. G.; Marshala, M.; Kelsh, L. *Bioorg. Med. Chem. Lett.* **1994**, *4*, 1999.

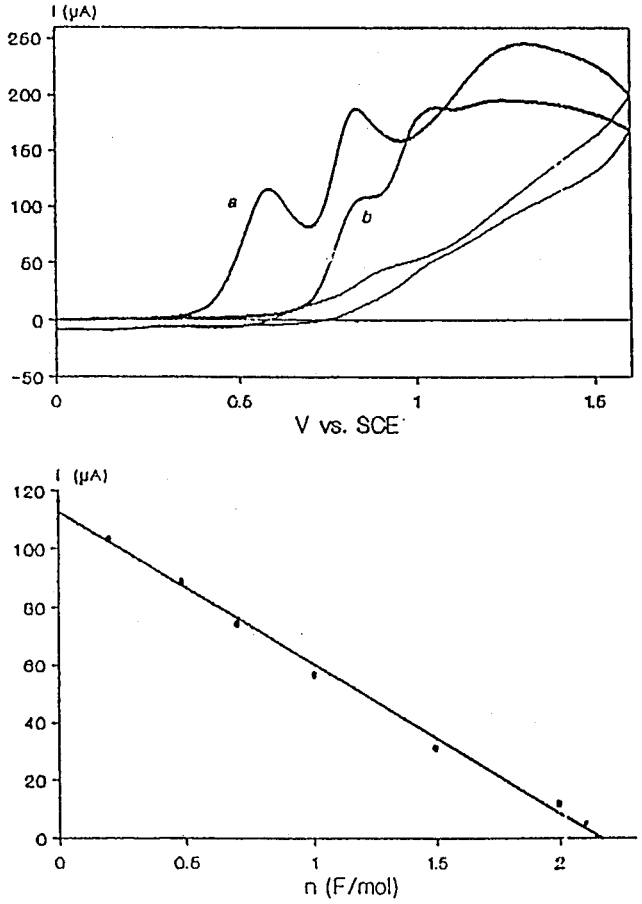


**Figure 5.** Top: Cyclic voltammograms in MeCN−0.1 M $Et_4NClO_4$ solution (50 mL) of $CathH^+$ (50.8 mg, 0.137 mmol) plus Vind (62.5 mg, 0.137 mmol) plus 2,6-lutidine (65 $\mu$L, 0.55 mmol) GCE; $v$ = 100 mV/s, (a) 0.0, (b) 2.0 F/mol. Bottom: Dependence of the peak currents on charge passed.

tion of 2 F/mol (Figure 5). The final step, $NaBH_4$ reduction, is carried out without isolation of $AVBL^+$, yielding anhydrovinblastine as mixture of natural (16′*S*)- and unnatural (16′*R*)-enantiomers in 4.3:1 ratio.

As depicted in Scheme 3, selectively controlled potential oxidation of Cath is occurring through two-electron oxidation and fragmentation of the C16−C21 bond, giving the pivotal dication **1a**$^{++}$ which subsequently undergoes a nucleophilic attack by Vind**.** The key result obtained in the anodic oxidation of catharanthine in the presence of vindoline is the preference for the 16′*S*-isomer at room temperature. This is the opposite of that observed for the Polanovski reaction in which the 16′*R*-isomer is formed at room temperature while below −40 °C the 16′*S*-isomer is favored as the primary product.[6b] It was suggested[8] that at low temperature a dication **1a**$^{++}$, retaining the original conformation of catharanthine, was produced and was nucleophilically attacked from the sterically hindered α-face leading to (16′*S*)-AVBL**.** At higher temperature, a conformational change takes place to give a dication which is attacked by vindoline from the $\beta$-face and after the reduction with $NaBH_4$ yields (16′*R*)-AVBL.

The favorable selectivity found in the electrochemical synthesis of AVBL, e.g. (16′*S*)-AVBL:(16′*R*)-AVBL is 4.3:1 at room temperature, can be rationalized by proposing that dication **1a**$^{++}$ is adsorbed to the electrode surface in a "tilted manner" and that electronic and steric requirements are such that the vindoline molecule must

**Scheme 3**

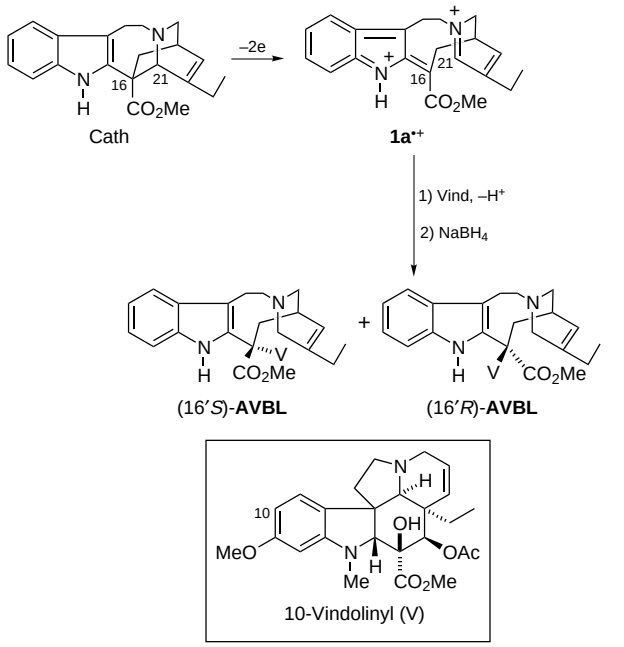


enter from the hindered α-face of the molecule thereby generating the natural configuration at C16. No attempts were made to optimize the stereoselectivity. However, we believe that changing of the reaction parameters (solvent, temperature, supporting electrolyte, electrode material, etc.) would improve the stereoselectivity of the reaction.

**Reaction Mechanism.** The most likely mechanism of the oxidation of catharanthine in the presence of vindoline, which fits the observed electrochemical and preparative results, is described in the form of Scheme 4.

In the rate-determining step catharanthine (Cath) is oxidized to the radical cation, $Cath^{\bullet+}$ (reaction 3). The irreversibility of this first electron transfer was proven experimentally by cyclic voltammetry and homogeneous redox catalysis. This process is accompanied with the changing of hybridization of the amine moiety from $sp^3$ in Cath to $sp^2$ in $Cath^{\bullet+}$.[23] Strain energy differences resulting from these geometrical preferences distort the preferred planar configuration thereby increasing the free energy for electron transfer. The flattening at the nitrogen is accompanied by an increase in the p character of the half-occupied orbital at the nitrogen. This results in an accumulation of strain in the molecule. Thus, the C16−C21 bond fragmentation reaction releases most of this strain in the transition state. The near-perfect alignment of $\sigma$-orbitals of the scissile bond with the $\pi$-system of the indole ring (vide infra ) would facilitate the fragmentation process leading to a new radical cation, **1a**$^{\bullet+}$ (reaction 4). The rate of the C16−C21 fragmentation reaction appeared to be solvent dependent. Our recent study on the fragmentation reaction in MeOH,[13] based on the value of the transfer coefficient determined in MeOH ($\alpha = 0.3$), showed that the Cath → **1a**$^{\bullet+}$ process is occurring through a concerted mechanism. The transfer coefficient determined in MeCN ($\alpha = 0.51$) suggests the "stepwise" process for reactions 3 and 4 (Scheme 4). It

(23) (a) Nelsen, S. F.; Blackstock, S. C.; Steffek, D. J.; Cunkle, G. T.; Kurzweil, M. L. *J. Am. Chem. Soc.* **1988**, *110*, 6199. (b) Nelsen, S. F.; Cuncle, G. T. *J. Org. Chem.* **1985**, *50*, 3701. (c) Nelsen, S. F. *J Org. Chem.* **1984**, *49*, 1891.

**Scheme 4**

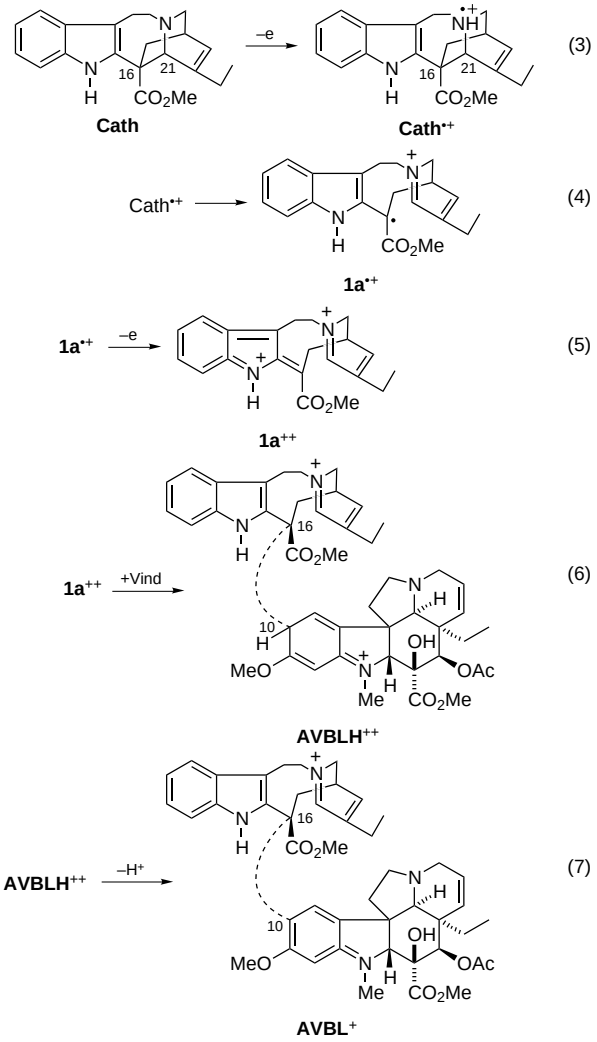


is possible that the solvation of the radical cation, **1a**$^{\bullet+}$, is more exergonic in MeOH than in MeCN, providing an additional driving force for the C16−C21 fragmentation reaction. Since the rate of the reaction 4 is fast, the radical cation **1a**$^{\bullet+}$ is formed close to the electrode surface and is oxidized at the applied potential to the dication **1a**$^{++}$ (reaction 5).

The nine-membered cyclic immonium ion **1a**$^{++}$ generated by anodic oxidation of Cath, is the same intermediate proposed in the Polanovski coupling reaction of catharanthine *N*-oxide with vindoline by trifluoroacetic anhydride.[6] In the mechanistic study of the Polanovski reaction, Sundberg and co-workers[8] found that the fragmentation of Cath is accelerated by Vind and other bases and the deprotonation of the indole nitrogen represented a reasonable mechanistic pathway for this catalysis. However, the fragmentation of *N*-methylcatharanthine is also accelerated by base, indicating that there must be a second aspect of base catalysis.[8]

Our experiments with cyclic voltammetry of Cath suggest that the overall rate of the fragmentation/coupling reaction is enhanced by the presence of Vind which is consistent with Sundberg's results.[8] The nucleophilic attack of Vind gives rise to the intermediate AVBLH$^{++}$ (reaction 6) which is deprotonated by 2,6-lutidine present as a base leading to AVBL$^{+}$ (reaction 7). We believe that reaction 7, which was not considered in Sundberg's mechanistic scheme,[8] is an important base-catalyzed reaction.

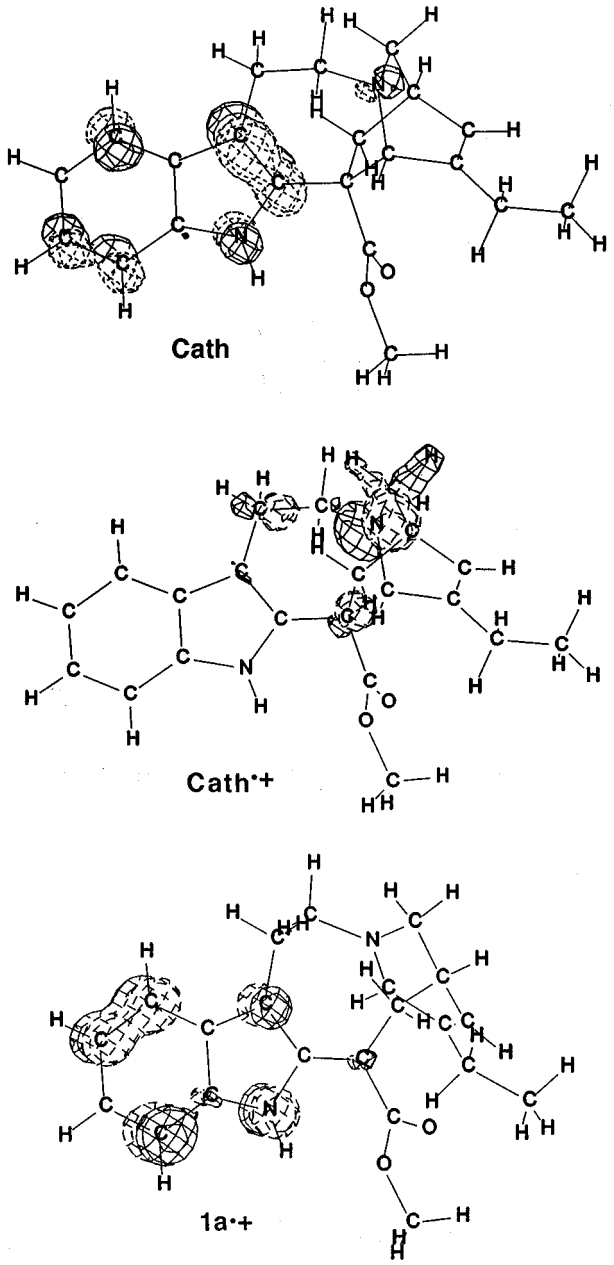


**Figure 6.** HOMO for Cath and SOMO for Cath$^{\bullet+}$ and **1a**$^{\bullet+}$.

**Table 2. Calculated Heats of Formation and Ionization Potentials**

| molecule | $\Delta H_f$ (kcal/mol) | IP (eV) | charge on N-4 |
|---|---|---|---|
| Cath | −7.449 | 8.311 | −0.2559 |
| Cath$^{\bullet+}$ | 161.656 | 12.346 | −0.2574 |
| **1a**$^{\bullet+}$ | 150.126 | | −0.1020 |

In order to explain the mechanistic problems in the anodic fragmentation of C16−C21 bond in Cath molecular orbital calculations of Cath, Cath$^{\bullet+}$, and **1a**$^{\bullet+}$ were carried out. Theoretical self-consistent field calculations were performed using the all-valence electron approximation by MNDO-AM1 method.[24,25] Some data on molecules and species are given in Table 2, and distribution of electron densities in the HOMO and SOMO orbitals are shown in Figure 6.

The results obtained by molecular orbital calculations support the proposed ECE mechanism (E is the first electron transfer, C is the C16−C21 bond fragmentation, E is the second electron transfer) in Scheme 4 (eqs 3−5).

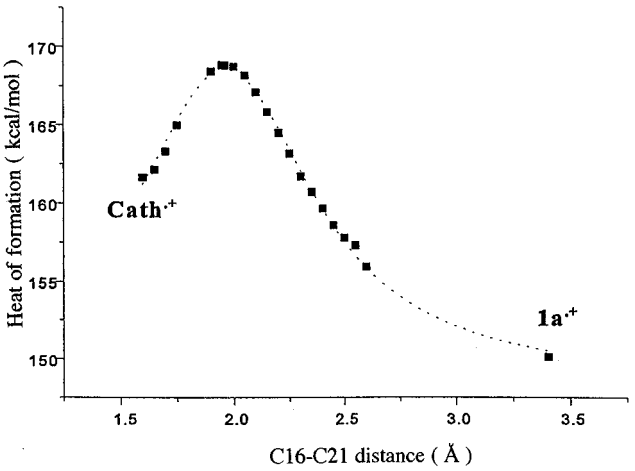


**Figure 7.** Calculated reaction path coordinate for C16−C21 bond fragmentation of Cath$^{\bullet+}$.

The chemical step which follows the electron transfer is the fragmentation of C16−C21 bond of the formed radical cation Cath$^{\bullet+}$ leading to the new radical cation **1a**$^{\bullet+}$. Inspection of bicentric energy terms for Cath$^{\bullet+}$ shows considerable differences in bond energies with the lowest energy for C16−C21 bond (12.048 eV) which means that the C16−C21 bond breaks more easily. The alternative EEC mechanism can be ruled out due to the very high oxidation potential of Cath$^{\bullet+}$ (IP = 12.346 eV) compared with Cath (IP = 8.311 eV). The unimolecular C16−C21 bond fragmentation may follow a homolytic or heterolytic mode. This depends mainly upon the relative stabilities of the formed indolyl (homolytic mode) or azaallyl radicals (heterolytic mode). MOPAC reaction path calculations employing Cath$^{\bullet+}$ were carried out to determine the barrier for C16−C21 bond fragmentation.[25] The energy profile for C16−C21 bond fragmentation is given in Figure 7.

The structure of the transition state is refined using TS option of MOPAC, and vibrational analysis was proven to be a genuine transition state having only one negative frequency. In the transition state the C16−C21 distance equals 1.963 Å, and $\Delta H_f$ = 168.838 kcal/mol. These calculations show that the homolytic mode of fragmentation of Cath$^{\bullet+}$ to **1a**$^{\bullet+}$ is favored. The optimized geometries for these isomers reveal that **1a**$^{\bullet+}$ is more stable by about 10.5 kcal/mol, providing a considerable driving force for the reaction. The activation barrier for C16−C21 fragmentation was about 7 kcal/mol.The distribution of electron densities and shape of SOMO orbitals of "transformed" radical cation **1a**$^{\bullet+}$ (Figure 6) shows that the spin density is located at the indole ring. Futhermore, the product obtained by photolysis of Cath in the presence of an electron acceptor[11a] indicates that the homolytic mode of C16−C21 bond fragmentation is more feasible.

## Experimental Section

**Chemicals and Apparatus.** Catharanthine hydrochloride and vindoline (Gideon Richter, Hungary), and $LiClO_4$ and 2,6-lutidine (Aldrich) were used as received. Acetonitrile (Aldrich, HPLC grade) was distilled over $CaH_2$ prior to use. $Et_4NClO_4$ (Aldrich) was recrystallized from water and dried. HPLC analysis were performed with Varian Vista 5500 equipment with UV-200 detector and integrator Varian 440 using micro column MCH-5N CAP (15 cm × 4 mm) at 284 nm with MeOH (0.5 mL/min) as an eluant.

**Electrochemistry.** The voltammetric mesurements were performed in a 25 mL conical cell with a glassy carbon electrode ($A$ = 0.071 cm$^2$) or platinum disc electrode ($2r$ = 1 mm), with platinum as a counter electrode and saturated calomel electrode (SCE) as a reference electrode. All electrochemical measurements were carried out using a PAR M-270-1 or PAR M-175 electrochemical analysis system. Preparative electrochemical synthesis of anhydrovinblastine was described earlier.[12]

**Modified Working Curves for Homogeneous Redox Catalysis.** Voltammograms were simulated using Digi Sim (version 2.1, Bioanalytical System) based upon the ECE mechanism of redox-catalyzed oxidation of catharanthine via the ferrocene/ferrocinium couple. The diffusion coefficients of ferrocene and ferrocinium ion were set equal to 2.4 × 10$^{-5}$ cm$^2$/s while those for all of the catharanthine species were assumed to equal that of catharanthine itself, 1.4 × 10$^{-5}$ cm$^2$/s. The rate constant for the reverse electron transfer reaction, $k_2$, was assumed to be at the diffusion-controlled limit, 10$^{10}$ M$^{-1}$ s$^{-1}$.

The rate constant for C16−C21 fragmentation reaction, $k$, was set at 10$^{10}$ s$^{-1}$ to insure that the working curves would correspond to the limit of rate control by the forward electron transfer, i.e. $k \gg k_2C^*_{Fc}$. Planar diffusion was assumed. The resulting curves differ significantly from those for the case of equal diffusion coefficients[19] particularly for large values of $\Lambda_1$ which corresponds to a large degree of catalysis.

**MO Calculations.** The MNDO procedure has proven to be reliable for studying molecular properties of heteronuclear radical in many previous studies.[24,25] The AM1 parametrization was used as more reliable for ionization potentials. We used the MOPAC program[24d] package, Version 7.01. Odd-electron systems were calculated by the "half-electron" method. The optimized geometries of all molecules were obtained by the force field minima in vacuum according to the AM1 method. Geometries of transition states were obtained using the reaction coordinate facility of MOPAC, and structure is refined using TS keyword.

**Acknowledgment.** The preparation of modified working curves for homogeneous redox catalysis described here were conducted at Department of Chemistry, University of Delaware. We are grateful to Edward W. Oliver for technical assistance. We wish to thank Professors Dennis H. Evans (University of Delaware) and Larry L. Miller (University of Minnesota) for their helpful discussions and support.

JO9621128

(24) (a) Bingham, R. C.; Dewar, M. J. S.; Lo, D. H. *J. Am. Chem. Soc.* **1975**, *97*, 1285. (b) Bischof, P. *Croat. Chem. Acta* **1980**, *53*, 51. (c) Dewar, M. J. S.; Ford, G.; Rzepa, H. S.; Yamaguchi, Y. *J. Mol. Struct.* **1978**, *43*, 1325. (d) Stewart, J. J. *QCPE* No. 455. (e) Rzepa, H. S.; Wylie, W. A. *J. Chem. Soc., Perkin Trans. 2* **1991**, 939.

(25) (a) Gano, J. E.; Jacob, F. J.; Roesner, R. *J. Comput. Chem.* **1991**, *12*, 127. (b) Smith, D. A.; Ulmer, C. W.; Gilbert, M. J. *J. Comput. Chem.* **1992**, *13*, 640.